



HAL
open science

A fast and accurate 1-dimensional model for dynamic simulation and optimization of a stratified thermal energy storage

Alix Untrau, Sabine Sochard, Frédéric Marias, Jean-Michel Reneaume, Galo A.C. Le Roux, Sylvain Serra

► To cite this version:

Alix Untrau, Sabine Sochard, Frédéric Marias, Jean-Michel Reneaume, Galo A.C. Le Roux, et al.. A fast and accurate 1-dimensional model for dynamic simulation and optimization of a stratified thermal energy storage. *Applied Energy*, 2023, 333, pp.120614. 10.1016/j.apenergy.2022.120614 . hal-03947326

HAL Id: hal-03947326

<https://univ-pau.hal.science/hal-03947326>

Submitted on 19 Jan 2023

HAL is a multi-disciplinary open access archive for the deposit and dissemination of scientific research documents, whether they are published or not. The documents may come from teaching and research institutions in France or abroad, or from public or private research centers.

L'archive ouverte pluridisciplinaire **HAL**, est destinée au dépôt et à la diffusion de documents scientifiques de niveau recherche, publiés ou non, émanant des établissements d'enseignement et de recherche français ou étrangers, des laboratoires publics ou privés.

A fast and accurate 1-dimensional model for dynamic simulation and optimization of a stratified thermal energy storage

Alix Untrau^{a,*}, Sabine Sochard^a, Frédéric Marias^a, Jean-Michel Reneaume^a,
Galo A.C. Le Roux^b, Sylvain Serra^a

^a*Universite de Pau et des Pays de l'Adour, E2S UPPA, LaTEP, Pau, France*

^b*Universidade de São Paulo, Escola Politécnica, São Paulo, Brasil*

Abstract

As renewable energies are incorporated in larger shares in the electricity grid and district heating and cooling networks, the integration of storage solutions becomes more important. Thermal Energy Storage is an effective way to store heat and utilize the synergies between different energy carriers. Stratified storage tanks are a promising technology because of their low cost, simplicity and reliability. However, the modeling of the thermocline region in a stratified tank remains a challenge. There is a need to develop a fast and accurate 1D model for simulations and optimizations of TES. In this paper, a new discretization scheme is applied to the vertical axis of the storage tank. Orthogonal Collocation accurately represents the temperature profiles inside the storage tank with less points than the traditional multinode model, therefore running faster. Oscillations appear in the temperature profiles computed with orthogonal collocation if the thermocline represented is too steep and a low number of discretization points is used. But if a realistic thermocline is used as initial condition, the model performs well. Thus, it is appropriate to represent the real behavior of a storage tank, where uniform temperature conditions are avoided. Orthogonal Collocation on Finite Elements runs even faster and represents a good perspective for optimization studies. The model developed in this paper is vali-

*alix.untrau@univ-pau.fr

dated with real data from a solar thermal plant with storage. A continuous and smooth model is also developed for natural convection inside the storage tank. The limitations of the model are discussed and perspectives on the modeling of natural convection for optimization models are given.

Keywords: Thermal Energy Storage, Modeling, Thermocline, Orthogonal Collocation, Optimization

Nomenclature

Abbreviations

CFD	Computational Fluid Dynamics
DHCN	District Heating and Cooling Network
MAE	Mean Absolute Error
MAPE	Mean Absolute Percentage Error
OC	Orthogonal Collocation
OCFE	Orthogonal Collocation on Finite Elements
TES	Thermal Energy Storage

Symbols

β	Thermal expansion coefficient [K^{-1}]
Δz	Tank layer height in the multinode model [m]
\dot{m}_c	Mass flow rate to charge the storage tank [$kg.s^{-1}$]
\dot{m}_d	Mass flow rate to discharge the storage tank [$kg.s^{-1}$]
ρ	Storage fluid density [$kg.m^{-3}$]
A	Tank cross sectional area [m^2]

a_i	Coefficient associated with the trial function f_i^{trial}
A_{OCFE}	Matrix representing the first derivative in the OCFE method
A_{OC}	Matrix representing the first derivative in the OC method
B_{OCFE}	Matrix representing the second derivative in the OCFE method
B_{OC}	Matrix representing the second derivative in the OC method
C_p	Storage fluid heat capacity [$J.kg^{-1}.K^{-1}$]
d_{insu}	Thickness of the insulation layer [m]
E	Energy stored inside the tank [J]
f_i^{trial}	Trial function in the OC formulation
g	Gravitational acceleration [$m.s^{-2}$]
H	Tank height
H_{ext}	Convection coefficient with the ambient air [$W.m^{-2}.K^{-1}$]
K	Von Karman constant
k^*	Effective thermal conductivity [$W.m^{-1}.K^{-1}$]
k_{fluid}	Thermal conductivity of the storage fluid [$W.m^{-1}.K^{-1}$]
k_{insu}	Thermal conductivity of the insulation layer [$W.m^{-1}.K^{-1}$]
k_{turb}	Turbulent diffusion coefficient [$W.m^{-1}.K^{-1}$]
k_{wall}	Thermal conductivity of the tank wall [$W.m^{-1}.K^{-1}$]
l_i	Lagrange polynomial
L_{el}	Length of an element in the OCFE method [m]
P	Tank perimeter [m]
R_{ext}	External radius of the storage tank [m]

R_{int}	Internal radius of the storage tank [m]
S_1	Exchanger surface between the bottom layer and the environment [m^2]
S_l	Lateral surface of a tank layer [m^2]
S_N	Exchanger surface between the top layer and the environment [m^2]
t	Time [s]
$T(z, t)$	Fluid temperature inside the tank [$^{\circ}C$]
$T_{amb}(t)$	Ambient temperature [$^{\circ}C$]
T_{charge}	Temperature of the charging fluid [$^{\circ}C$]
T_{return}	Cold temperature returning to the storage tank [$^{\circ}C$]
U	Tank fluid to ambient overall heat transfer coefficient [$W.m^{-2}.K^{-1}$]
U_1	Tank fluid to ambient overall heat transfer coefficient for the bottom layer [$W.m^{-2}.K^{-1}$]
U_N	Tank fluid to ambient overall heat transfer coefficient for the top layer [$W.m^{-2}.K^{-1}$]
z	Tank height from the bottom of the tank [m]

1. Introduction

In order to reduce the green house gases emissions of the energy sector, renewable energies will be incorporated in greater share into the electricity grid and District Heating and Cooling Networks (DHCN) [1]. Some of these renewable energies are intermittent, such as wind or solar energy. Thus, storage of the energy produced is required to ensure that the energy demand is met. Heat can be stored easily, unlike electricity [2]. Therefore, Thermal Energy Storage

(TES) is an important technology to develop. TES can be used to store hot fluid for space heating, domestic hot water or industrial processes. Moreover, if the temperature of the stored fluid is high enough, steam and electricity can be generated with the hot fluid. TES allows to exploit the synergies between heat and electricity [3]. Thus, TES can be used in association with solar thermal plants or conventional thermal plants in order to store the heat produced. This will help to overcome the intermittency of renewable energies and will ensure that the energy demand is met.

There are three categories of TES based on different phenomena to store the heat: sensible, latent and thermochemical [4]. The design, modeling and optimization of all types of technologies are studied actively nowadays. For example, a packed bed sensible heat storage was investigated in [5], a latent heat storage included in a solar system was optimized [6], and an adsorption heat storage was modeled in [7]. Hybrid storage solutions, such as a stratified storage tank with phase change emulsion in [8], are also explored and simulation models are developed. Although latent and thermochemical storage technologies are promising, sensible heat storage is mostly used nowadays, because of its low cost, reliability and high level of maturity. There are two main ways to store the sensible heat in a thermal plant. It is possible to use two storage tanks, one for the hot fluid exiting the plant and one for the cold fluid returning to the plant, such as in [9]. The second option takes advantage of thermal stratification. It uses one single tank that is charged from the top with hot fluid while the cold fluid returning to the plant is charged from the bottom [10]. Because the density of the storage fluid is lower at higher temperatures, there is no significant mixing taking place between the hot and cold zones. The temperature gradient between these two zones is very steep and this region is called the thermocline. The stratification inside the storage tank is illustrated in Figure 1. This figure shows the thermocline region and the temperature profile inside the storage tank as an example.

This single tank technology is cheaper to build because it requires less land space and construction materials, and is less complex [11]. For low tempera-

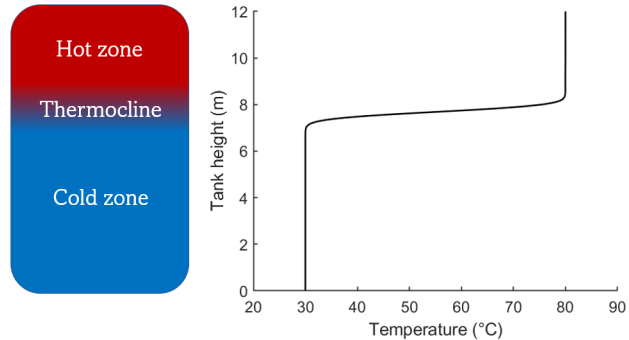


Figure 1: The thermocline region and the temperature profile inside the tank

tures, water is a commonly used storage fluid because of its availability and low cost. For application at higher temperatures, other fluids are chosen, such as molten salts for example, and packed bed materials, such as rocks, metals, ceramics or recycled materials are added [12]. Naturally stratified storage tanks and thermocline storages with filler material share common features. In both technologies, a thermocline separates a cold and a hot zone, and can be thickened due to diffusion and convection [13]. However, the filler material plays a role in destratification. If idle periods are long, both water and bed conductivity lead to thermocline thickening [14]. Moreover, the limited heat transfer between the fluid and the filler material can also lead to thermal destratification. The present paper focuses on naturally stratified water storage tanks without any filler material. However, the model proposed in this work could be adapted to packed bed thermocline storages. The storage tank used for an energy system can be long-term, also called seasonal storage, to store heat between seasons. The other type of storage tank is short-term or daily, to store between days. This paper focuses on short term storage tanks, although the model developed in this work could also be applied to seasonal storage tanks.

Developing fast and accurate simulation and optimization models of TES is crucial to accelerate their integration in smart grids or DHCN. Especially, TES models for real-time optimization and control of energy systems, such as solar

thermal plants [15], are needed. Since they will be used online, they need to run even faster than offline optimization models. The modeling of thermocline TES requires spatial discretization, which can lead to complex and computationally expensive models. 3D and 2D approaches are useful to understand the phenomena taking place inside the storage tank but optimization studies or simulation studies of larger systems require a 1D model to speed up calculations. In the tank, a temperature inversion might arise if the storage is charged with a lower temperature, or because of heat losses for example. This is rapidly corrected by natural convection in the real system. However, the 1D model does not traditionally include a natural convection term. It needs to be added in order to correct temperature inversions. Adding the modeling of this 3D phenomenon in a 1D model remains a challenge. In this paper, a new discretization scheme for a 1D model, based on orthogonal collocation, is presented. This model is able to represent more accurately the thermocline region than the finite volumes discretization scheme that is traditionally used, and with reduced computational time. Some perspectives on the modeling of natural convection in a 1D model are also provided.

This paper is divided as follows: Section 2 presents the state of the art of TES modeling. Section 3 details the traditional 1D model based on finite volumes and its drawbacks. Section 4 introduces orthogonal collocation and its application for the spatial discretization of TES. Section 5 shows the results obtained with the new discretization scheme. It also compares the two previously mentioned schemes, in terms of the estimation of the temperature profile in the storage tank as well as the valuable stored energy. Section 6 introduces the adapted discretization scheme for optimization, Orthogonal Collocation on Finite Elements, and provides more results on the modeling of the TES in operation. Finally, Section 7 is the validation of the model with real plant data and Section 8 briefly discusses natural convection modeling.

2. Literature review on stratified TES modeling

In a thermocline storage tank, it is crucial to maintain the best degree of stratification possible, which means that the thermocline must remain as thin as possible. Indeed, if there is some mixing between the hot fluid and the cold fluid, it will deteriorate the energy stored at the top of the tank by decreasing its temperature. Several phenomena lead to destratification inside the storage tank: the mixing induced during charging and discharging, the vertical diffusion between the hot and cold zones, natural convection due to charging and discharging at a variable temperature and to heat losses to the environment [16]. He *et al.* [11] analysed experimentally the thermocline evolution inside a storage tank during charging and discharging and also during the static mode. They observed that long periods of stand-by status should be avoided because the thermocline widens with diffusion. Also, the thermocline thickness is highly dependant on the flow rate during the charging and discharging phases. New technologies are developed to enable a better stratification inside the TES, focusing on the inlet design and location. For example, in [17], a thin flexible tube, called water snake, delivers the incoming fluid in the TES at the position in the tank where the temperature and density of the stored fluid and the incoming fluid are the same. This minimizes mixing and turbulence inside the TES. Although promising, this design is still in the early stages of development.

Modeling a thermocline storage tank is challenging. The thermocline must be represented accurately because the temperature gradient in this region is very steep. On the other hand, the integration of a TES model into a thermal plant model or an energy network leads to long computational time. Therefore, it is necessary to find a compromise between computational time and accurate estimation of the valuable energy stored inside the storage tank. The compromise is even more necessary for real-applications, such as real-time optimization and control. Depending on the study objective, various modeling techniques have been developed, summarized in [18] for example, and explained below.

TES can be modelled in 3D, using Computational Fluid Dynamics (CFD)

for example, in order to accurately represent all the phenomena taking place inside the tank. In such models, the mass, momentum and energy balance equations are solved on a 3D grid. These models allow to understand better the fluid movements around the diffusers for instance [19], in order to improve their design and maintain a better stratification. Natural convection, taking place when temperature inversions appear inside the tank, can also be studied. Buoyancy forces due to natural convection correct these temperature inversions in a few minutes. For example, the transient cooling inside the storage tank and the natural convection movement induced by sidewall heat losses were investigated with CFD in [20]. 3D and 2D CFD models are very accurate but also computationally expensive. For storage tanks, a 2D simulation of the symmetry plane might help to reduce the computational burden, such as in [8], but further reduction in computational time may be necessary for some applications. Thus, 2D and 3D models are usually employed to improve the design of TES (in [21] for example) or to validate simplified models. Indeed, simplified models are needed for long term simulations, complex energy systems simulations or optimization studies. For instance, Johannes *et al.* [22] used a CFD model with 110,000 nodes to model a TES and noticed a bi-dimensional mass transfer leading to a non-uniform temperature along the radial axis of the tank. Their accurate model was used to validate a simplified 1D model along experimental measurements. They found a good agreement between the two models and the experiments for the vertical temperature profiles inside the storage tank. Thus, they suggested to use the 1D model for the simulation of a global energy system.

2D zonal models allow the modeling of a temperature gradient in the radial direction with shorter computational times than CFD because they do not solve the momentum equation. Nevertheless, they can still be computationally expensive and are used as references to validate 1D models (in [23] for example). De Césaro Oliveski *et al.* [23] concluded that their 1D model is much faster than the reference 2D model and the two models are in good agreement for the representation of the vertical temperature profiles inside the storage tank. Therefore, it is not necessary to use a 2D model for long-term simulations.

For optimization studies of energy systems, it is more common to use a 1D model for the TES. In this case, only the temperature variations along the vertical axis are considered. We assume that there is no temperature gradient in the radial direction. This assumption has been verified experimentally, in [24] for instance, in which the radial temperature gradients measured were below 1°C . The 1D model is a good approximation when the storage tank is cylindrical with its inlet and outlet located at the top and bottom surfaces on the axis of symmetry [25]. For other geometries, the 1D approximation is less accurate. The simplest 1D model is the fully-mixed storage tank. The temperature is assumed uniform inside the whole storage tank, and there is no stratification. This model leads to an important exergy destruction [26]. The ideally stratified storage tank considers two zones with fixed temperatures and variable volumes, one for the cold fluid and one for the hot fluid. The thermocline is considered having a zero thickness and moves up and down along the vertical axis of the tank. This model overestimates the valuable energy stored by considering a perfect stratification [26]. In [27] two layers with variable volumes and temperatures were modeled and a hypothetical transition profile of the temperature, centered in the ideal separation line, was added to reproduce the thermocline. This model still runs fast but is more accurate than the ideally stratified storage tank model. The plug flow model uses a variable number of layers of fluid, each with a variable volume [16]. A new layer is added when the incoming fluid temperature (during the charge or discharge) is too different from the closest layer temperature (more than 0.5°C difference). Otherwise, the incoming fluid is mixed with the fluid from the closest layer. The temperature profile is then shifted and the volume of fluid crossing the boundary of the storage tank is sent back to the heat source or sink. This 1D model is fast but does not rely on mass and energy balances and therefore, it is not very accurate. The last 1D model strategy is to solve the energy balance in the storage tank along an ascending vertical axis z . Assuming constant thermophysical properties for the storage fluid and no heat source inside the storage tank, the conservation of energy in 1D over a control volume of thickness dz leads to the following Partial Differential Equation (PDE):

$$\rho C_p A \frac{\partial T(z,t)}{\partial t} + \dot{m} C_p \frac{\partial T(z,t)}{\partial z} = Ak \frac{\partial^2 T(z,t)}{\partial z^2} + UP(T_{amb}(t) - T(z,t)) \quad (1)$$

The first term is the energy accumulation, the second term represents the enthalpy fluxes due to the charge or discharge, the third term represents diffusion inside the tank and the final term models the heat losses to the environment. In Equation 1, the unknown variable is the storage fluid temperature $T(z,t)$ varying in space, along the vertical coordinate z , and in time t . ρ represents the stored fluid density, C_p the stored fluid heat capacity and k the stored fluid thermal conductivity. They are all assumed uniform and constant. A is the tank cross-sectional area, P is its perimeter. The enthalpy fluxes due to charge or discharge depend on the resulting flow rate \dot{m} inside the storage tank. The thermal losses are computed based on an overall heat transfer coefficient U between the tank fluid and the ambient air at the temperature T_{amb} . Details on how we computed U in our model are given in Section 3. The variables and parameters involved in Equation 1 are listed in the nomenclature.

The initial condition for the temperature in Equation 1 could be either a fully mixed condition, represented by a single uniform temperature, or a known temperature gradient [28].

The boundary conditions at the top and bottom of the storage tank depend on its utilization ([29], [30]):

- Charge : $\left. \frac{\partial T(z,t)}{\partial z} \right|_{z=0} = 0$; $T_{z=H} = T_{charge}$
- Discharge : $T_{z=0} = T_{return}$; $\left. \frac{\partial T(z,t)}{\partial z} \right|_{z=H} = 0$
- Idle period : $\left. \frac{\partial T(z,t)}{\partial z} \right|_{z=0} = 0$; $\left. \frac{\partial T(z,t)}{\partial z} \right|_{z=H} = 0$

In these equations, $z = 0$ is the bottom of the storage tank, while $z = H$ is the top of the storage tank of height H . T_{charge} and T_{return} are the temperatures respectively of the charging flow and the return flow. When fluid is entering the tank, the temperature at the inlet of the storage is equal to the incoming fluid temperature. When fluid is leaving the tank, which corresponds to the bottom

during charge and the top during discharge, a zero gradient is considered for the temperature. It means that the fluid at the outlet is at the same temperature on each side of the outlet (storage side and pipe side). During idle periods, the temperature gradient is also considered zero, which means that an adiabatic surface is assumed. A value could be given to the temperature gradient, equal to the heat losses to the environment through the top and bottom surfaces of the tank. Fixed boundary conditions can only be applied if a fixed working mode is determined for the simulation study. Otherwise, strategies need to be developed to represent the changing boundary conditions. This will be explored in 4.3.

In order to solve this EDP, different discretization strategies along the space variable z can be used. They will allow the transformation of the EDP into a system of Ordinary Differential Equations (ODE). The traditional discretization scheme is based on finite volumes and is called the multinode model. It relies on the division of the storage vertical axis into several layers of fixed height and uniform temperature. An energy balance is written for each layer. Its implementation will be detailed in the next section of the paper. The multinode model has often been used in recent works for various applications. Firstly, the stratified storage tank alone has been studied. This allowed to better understand its stratification evolution [31], assess its efficiency [32] and study the effect of the variation of important parameters on the TES performances [33]. Adaptations were made to the original formulation to incorporate immersed heat exchangers in [34]. This new model was then used to size the storage tank using deep learning methods [35]. Furthermore, the multinode model has been used to model the storage tank in a more complex energy system such as a micro-combined heat and power system [36], a solar district heating system [37] or a domestic hot water heat pump [38]. The authors sometimes implement the model themselves or directly use it within a software library, such as the TES implemented in TRNSYS used in [32], [26] and [39]. The model was also adapted in 2D for a seasonal pit storage in [40] with segments of equal volumes instead of equal height. Finally, the multinode model has been compared to fully-mixed

and ideally stratified models, showing a better estimation of the exergy stored [26]. Also, it has been compared to a 2D zonal model in [23] and a CFD model in [22], showing sufficient accuracy in the vertical temperature profiles with a greatly reduced computational time. As this literature review shows, the multinode model has been extensively studied and used in the recent years. Nevertheless, it presents the issue of numerical diffusion, a smoothing effect on the vertical temperature profile when a reduced number of nodes is used [41]. To overcome this issue, a large number of nodes needs to be used, at least 100 according to [27], making the computational time prohibitive for some applications. For the simulation of a complex system or an optimization, a reduced number of nodes is used, leading to poor accuracy. For example 60 nodes were used in [36], 26 nodes in [37], 15 nodes in [39] and 10 nodes in [34], [35] and [42]. These studies would benefit from a fast and accurate 1D model suitable for long-term simulations, global energy systems simulations and optimizations. A new discretization scheme, Orthogonal Collocation (OC), is introduced in Section 4 to resolve the issue of numerical diffusion. OC has never been applied to discretize the vertical axis of the storage tank. Other discretization schemes for Equation 1 have not been found in the literature. In [43], a 1D model with 5 layers of variable height but fixed temperatures was used for the incorporation of a TES in a MILP-based energy management system. In the present paper, no linearization is done and Equation 1 is directly solved.

An important aspect of a storage tank model connected to a thermal plant that does not work with a constant outlet temperature is the correction of temperature inversions. This is needed when working with a solar thermal plant for example. At the end of the day, the solar irradiation goes down and the temperature at the outlet of the solar field might decrease a few degrees. Nevertheless, the temperature reached is still high enough for the consumer needs and it might be interesting to store this fluid. In this scenario, the incoming fluid is slightly colder than the stored fluid at the top of the storage tank. A temperature inversion appears. In the real system, this temperature inversion will be corrected by buoyancy forces induced by natural convection. This mixing

phenomenon should be incorporated into the storage tank model [16]. Another cause for a temperature inversion is the heat losses that are more important along the walls of the storage tank, and especially on the top surface, where the area is the largest and the fluid is the hottest. The top section of fluid might cool down more rapidly than the rest of the stored fluid and therefore, a temperature inversion will appear [23]. Temperature inversions are the main cause for destratification [44]. Natural convection is a 3D phenomenon and its modeling requires the development of the momentum equation. The colder fluid entering the top of the tank will sink inside the tank because of its higher density. During its descent, it will exchange mass and energy with its surrounding, composed of warmer stored fluid. Thus, it will warm up and its downwards trajectory will stop once the temperature equilibrium is reached [24]. Therefore, the incoming fluid won't mix perfectly with the fluid at the top of the tank and it won't go to the zone of storage with the same temperature without affecting the stored fluid either. Different numerical artifices have been developed to model natural convection in 1D, and have generally been incorporated into the multinode model. The first category of methods is to perform an operation after each time step, if a temperature inversion is spotted inside the storage tank. The first method is to reorganize the temperatures after each time step, making sure that the hottest temperature is at the top of the storage tank and that the coldest is at the bottom [45]. This leads to an overestimation of the valuable stored energy because it neglects the mixing between the incoming fluid and the surrounding stored fluid. The other approach is to homogenize the temperatures around the inversion. A weighted mean temperature among the segments involved in the inversion is used [46]. These two methods provide good results [23] but require conditional structures to activate the operation only if needed. This is not easy to integrate into an optimization model because it only includes algebraic equations. Another method used in some studies is to inject the fluid inside the layer with the temperature closest to the charging temperature, thereby avoiding temperature inversions. Some actual systems provide several inlet ports to reproduce this behavior, but they are more expensive. Moreover, they do

not completely prevent temperature inversions as small temperature differences will still occur because there are only a few inlet ports or because of the heat losses through the top and lateral walls during idle periods. If the actual system has only one inlet at the top of the tank, injecting at a variable height in the model neglects the mass and energy transfer between the incoming and the stored fluids. Thus, it overestimates the performances of the storage tank [24]. Moreover, it requires the use of conditional structures and is not appropriate for optimization studies. Saloux *et al.* [47] developed an advanced flow rate distribution method to reproduce the mixing between the incoming and stored fluid during the incoming fluid descent through the storage tank. The method is based on heuristics and not on physical models. Pate developed a 1D model based on physical equations to describe the natural convection inside the storage tank [24]. It is called the plume entrainment model. Pate performed some experiments to visualize the trajectory of the incoming colder fluid. He observed that the colder fluid sinks inside the storage tank and some of the stored fluid is entrained with it. Some warmer stored fluid then rises inside the tank to replace the entrained fluid. Those turbulent movements are in 3D but the radial temperature gradient is negligible. From these observations, Pate developed a 1D plume entrainment model. Mass and energy balances are written for the plume and the bulk fluids. The plume stops its course when temperature equilibrium is reached. These differential equations have been solved with finite volumes and led to good results, in agreement with experimental results [24]. In order to solve the ODE system, the equations for the plume and the bulk were decoupled. The plume temperature was obtained from the previous bulk temperatures, and then the new bulk temperatures were computed using the plume depth ([44], [16]). Analytical solutions have also been developed, neglecting the diffusion term [25]. Although this model is promising since it is based on physics and is written in the form of ODEs, it is not appropriate for optimization studies because of the discontinuities in the flow rates computed inside the storage tank. Another approach is to model a turbulent diffusion coefficient that is large only when a temperature inversion appears ([28], [48],

[41], [49], [50]). The diffusion term in Equation 1 is then replaced by:

$$(k^* + k_{turb}) \frac{\partial^2 T(z, t)}{\partial z^2} \quad (2)$$

There are many formulations for the turbulent diffusion coefficient, based on physical models [28] or not, which must be several order or magnitudes larger than k^* [41]. This formulation requires a conditional structure to determine if k_{turb} is zero or not, but it is a continuous formulation that does not need to be performed at the end of each time step. For this reason, it is easier to incorporate into a simulation model using an automatic integrator. It is possible to transform this model into a smooth model by using a continuous approximation of the condition (logistic function for example) or the max function. The development of a continuous and smooth model for a storage tank with temperature inversion correction is the topic of very recent works ([51], [52]). These formulations are appropriate for optimization studies but they require the tuning of the smooth functions parameters to find the best compromise between accuracy and convergence ease. Finally, a different approach was presented in [53]. Inversion flow rates are introduced as optimization variables in the optimization problem. They are activated to minimize the temperature inversion sum, that is included in the objective function. This method also requires some tuning for the bounds on these flow rates and on the weight associated with the temperature inversion sum in the objective function. This approach is easy to implement in an optimization study and does not cause convergence difficulties.

Based on this literature survey, there is still a need to develop a fast and accurate 1D model for simulation and optimization studies. Moreover, ways to correct temperature inversions in an easy way are needed, especially for optimization models. This paper presents the discretization of the 1D model with orthogonal collocation, which has never been applied to this problem before. The model proposed hereafter requires less discretization points than the traditional multinode model to achieve the same accuracy. It is therefore faster to run. A discussion on how to model natural convection for optimization studies is added at the end of the paper.

3. Traditional one-dimensional model

3.1. Mathematical Formulation

In the traditional multinode model, Equation 1 is discretized with finite volumes, considering N layers of height Δz . Layer 1 is located at the bottom of the tank and layer N is located at the top. The unknown temperatures are located in the middle of each layer, and the temperature inside each layer is assumed uniform. This discretization scheme is illustrated in Figure 2, with the vertical axis named x and pointing upwards.

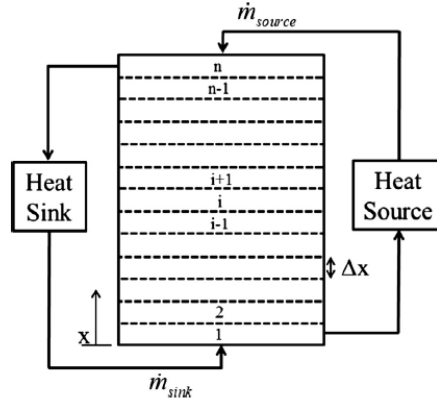


Figure 2: Finite volumes discretization scheme for TES [41]

Each layer is composed of the stored fluid and the wall, assumed in thermal equilibrium. The assumption stems from the large heat transfer coefficient between the stored water and the wall as well as the small thickness of the wall and its large conductivity. Thus, diffusion through the wall and convection in the water side are considered large, and the wall and the stored fluid are at the same temperature. In this discretization model, the first derivative with respect to z is approximated with finite differences of order 1 and used for the convective terms. The second derivative with respect to z is computed with centered finite differences, of order 2, and used for the diffusion term. For the top and bottom layers, the finite differences to approximate the second derivative are not centered but are computed using the wall temperature as one of the

neighbor temperatures. We assumed that the wall temperature is equal to the fluid temperature. Since the wall is located at the distance $\frac{\Delta z}{2}$ from the top and bottom, a coefficient of $\frac{4}{3}$ appear in front of the diffusion term for the top and bottom layers. The equations used for the different layers i , at the temperature T_i , are presented hereafter:

For the first layer at the bottom of the storage tank:

$$\rho C_p A \Delta z \frac{dT_1}{dt} = U_1 S_1 (T_{amb} - T_1) + \frac{4}{3} \frac{k^* A}{\Delta z} (T_2 - T_1) + \dot{m}_c C_p (T_2 - T_1) + \dot{m}_d C_p (T_{return} - T_1) \quad (3)$$

For an intermediate layer i , for i varying from 2 to $N-1$:

$$\rho C_p A \Delta z \frac{dT_i}{dt} = U_i S_i (T_{amb} - T_i) + \frac{k^* A}{\Delta z} (T_{i-1} - 2T_i + T_{i+1}) + \dot{m}_c C_p (T_{i+1} - T_i) + \dot{m}_d C_p (T_{i-1} - T_i) \quad (4)$$

For the last layer N at the top of the storage tank:

$$\rho C_p A \Delta z \frac{dT_N}{dt} = U_N S_N (T_{amb} - T_N) + \frac{4}{3} \frac{k^* A}{\Delta z} (T_{N-1} - T_N) + \dot{m}_c C_p (T_{charge} - T_N) + \dot{m}_d C_p (T_{N-1} - T_N) \quad (5)$$

The time dependency of the variables in these equations is not written for conciseness. In these equations, \dot{m}_c and \dot{m}_d are the flow rates of charge and discharge respectively. The temperature of charge T_{charge} and the return temperature T_{return} are the other inputs of the system. S_1 and S_N are the surfaces of the layers 1 and N respectively in contact with the ambient temperature. They are composed of the lateral surface of the tank layer as well as the top or bottom surface. Therefore, the heat losses are more important for these layers than the interior ones, because the exchange surface is larger.

The overall heat transfer coefficient with the environment takes into account the diffusion through the insulation layer of the storage tank (with a depth d_{insu} and a thermal conductivity k_{insu}) and the convection with the ambient air:

$$\frac{1}{U} = \frac{1}{H_{ext}} + \frac{d_{insu}}{k_{insu}} \quad (6)$$

The heat transfer coefficient with the environment H_{ext} can be determined with an experimental correlation and depends on the environmental conditions (wind speed for example). Thus, this coefficient is variable and depends on the weather. This coefficient can be different for the top, bottom and lateral surface (hence the different names U_1 , U and U_N in the above equations).

The effective thermal conductivity of the fluid and the wall is computed as follows:

$$k^* = k_{fluid} + k_{wall} \frac{R_{ext}^2 - R_{int}^2}{R_{int}^2} \quad (7)$$

In Equation 7, R_{ext} is the external radius of the storage tank, including the wall, while R_{int} is the internal radius only considering the fluid. The effective conductivity represents the effect of diffusion in the tank wall on the destratification [54]. Although the cross sectional area of the wall is much smaller than of the fluid, the large conductivity of the metallic wall contributes to the homogenization of the temperatures inside the storage tank. The thermal capacity mC_p is the one of the water only because the thermal capacity of the wall is neglected. Indeed, the specific heat capacity of the wall is small compared to the one of water and the mass of metal is much smaller than the mass of water.

3.2. Numerical Diffusion

One of the main assumptions in this model is the uniform temperature in each layer of fluid, which corresponds to an infinite thermal diffusion inside each layer. This generates an effect called numerical diffusion [41], where the temperature profile along the vertical axis of the tank is smoothed. This effect is highly dependent on the number of layers used in the model. If a large number of layers is used, the thermocline region will be represented more accurately but the computational time will be longer. This is illustrated in Figure 3 for 10, 100 and 1000 layers. In this example, a water storage tank of $500m^3$, initially at $30^\circ C$, was charged with hot fluid at $80^\circ C$ at a flow rate of $10kg.s^{-1}$. The charge was performed over 26 hours in order to completely fill the storage tank. The computational times were 0.1s, 0.14s and 4.7s for 10, 100 and 1000 layers respectively, on a laptop with the following characteristics: Intel Core i7-1065G7

1.3GHz, RAM 16Go. The simulation was performed on MATLAB and the solver ode15s was used for the time integration.

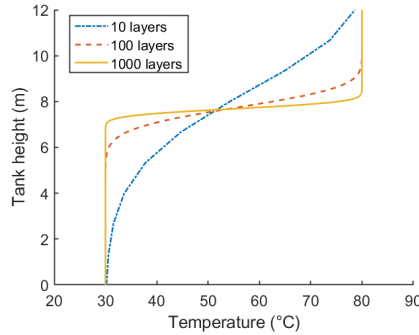


Figure 3: Impact of the number of layers on the temperature profiles

Figure 3 shows that the thermoclines are not well represented with a small number of layers. 1000 layers is not the converged solution yet and the thermocline continues to get thinner as the number of layers increases. Powell *et al.* [41] tested up to 10,000 layers and showed an improvement compared to 1000 layers. However, the computational time greatly increases with the number of layers and the model with 1000 is already about 30 times slower than the model with 100 layers. Thus, it is needed to find a compromise between the accuracy of the model and the computational time for complex long-term simulations and optimizations. For a study on the storage tank only, a large number of nodes can probably be used without making the computational time prohibitive. The bad representation of the thermocline region with a low number of layers has a direct impact on the quantity of energy stored at a temperature high enough for its utilization. The stored energy $E(t)$ at each time instant compared to the initial state of the storage tank is defined as follows:

$$E(t) = \int_{z=0}^{z=H} \rho AC_p (T(z, t) - T(z, 0)) dz \quad (8)$$

In this equation, $T(z, t)$ is the current temperature profile along the vertical axis inside the storage tank and $T(z, 0)$ is the initial profile acting as a reference. For an energy system, the quantity of energy stored is not the only variable of

interest, but also its temperature. For example, if the consumer requires heat at a minimum temperature of 65°C , then it is the quantity of stored energy with a temperature higher than 65°C that matters. A bad representation of the thermocline region does not affect the quantity of stored energy but its quality.

Figure 4 shows the cumulated energy at a temperature above 65°C stored throughout time during a charging phase, for different numbers of layers in the model. It can be observed that there is a large discrepancy between the cumulated energy profiles for 10 layers and for 100 or 1000 layers. A model with only 10 layers greatly underestimates storage utilization. Using 100 layers is a reasonable approximation, even if numerical diffusion still has an effect. A quantitative analysis shows that the maximal difference between the energy profile with 1000 layers and the one with 10 layers is 5.1MWh, while it is 1.3MWh for 100 layers. At the beginning of the charging phase, during the first hour, when the stored energy is small, the relative difference between the models with 1000 layers and 10 layers goes up to 100%, while it reaches 26% for 100 layers. This analysis shows that a bad representation of the thermoclines due to numerical diffusion with a model with few layers has a large impact on the estimation of the valuable stored energy. Furthermore, the time needed to completely charge the storage tank depends on its discretization. It takes 15 hours to completely charge the storage tank with the 1000 layers model while it takes 22 hours to do it with the 10 layers model. Therefore, using the multinode model with a small number of layers leads to an underestimation of the performances of the storage tank.

Modi *et al.* [33] chose to use 1500 layers after performing a grid convergence study for their packed bed storage tank. Their model was validated with experimental results. Mawire *et al.* [31] used 200 layers to model their TES because no further improvement was observed with a finer spatial grid. Aguilar *et al.* [38] used 100 layers and observed a deviation of 0.1% in the temperatures and energies computed compared to a model with 500 layers. These models used a large number of layers because they focused on the simulation of the storage tank only or on a simple system. The computational time was not an issue in

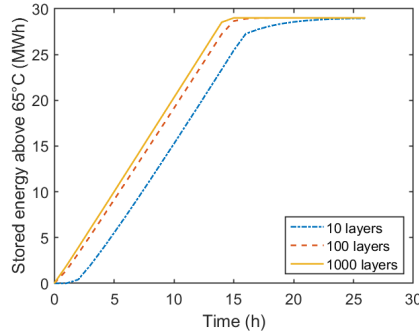


Figure 4: Cumulated stored energy through time during charging

these papers, and thus the authors were able to use enough discretization points to limit the numerical diffusion effect. For more complex systems, the number of layers needs to be reduced in order to achieve reasonable computational time. Thus, 60 layers were used for the TES in a micro-combined heat and power system [36], 15 layers were used for the TES associated with a ground source heat pump [39] and 10 layers were used for the TES with two immersed heat exchangers, whose model was developed in [34]. For the optimization of a complex energy system the number of layers must be further reduced to speed up the calculations. For instance, Socolan *et al.* [42] optimized the operation of a solar thermal plant including a storage tank. They used only 10 layers to model their storage tank. Similarly, Saloux *et al.* [37] minimized the primary energy used in a solar district heating system with a 26 layers TES model. The TES size was optimized in [35] with a model consisting of 10 layers. Although not very accurate, these models allowed the authors to obtain approximate results in a reasonable time. This highlights the need to develop a fast and accurate 1D TES model for complex long-term simulations or optimizations.

A first attempt to improve the results obtained was conducted in the present work. In the original method, the enthalpy fluxes associated with charging and discharging were computed with finite volumes in Equation 4, as shown below for the interior points:

$$\dot{m}_c C_p (T_{i+1} - T_i) + \dot{m}_d C_p (T_{i-1} - T_i) \quad (9)$$

This corresponds to a finite difference of order 1 to approximate the first derivative with respect to z .

These terms were replaced by the following, based on finite differences with a centered scheme, which corresponds to a finite difference of order 2 to approximate the first derivative with respect to z :

$$\frac{\dot{m}_c C_p (T_{i+1} - T_{i-1})}{2} + \frac{\dot{m}_d C_p (T_{i-1} - T_{i+1})}{2} \quad (10)$$

The centered scheme for the computation of the first derivative of the temperature could lead to more accurate results since it involves two neighbors temperatures instead of one, and the order of the finite difference was increased by 1. A simulation with 100 discretization points is performed for the charging phase presented previously. For the boundary conditions, the temperature at the top of the storage tank is equal to the charging temperature and the temperature at the bottom of the tank, which is where the fluid exits during a charging phase, has a zero spatial derivative [29]. The temperature profiles obtained are plotted in Figure 5, at four time instants. In this figure, the thermoclines are a bit steeper than the ones obtained with the traditional multinode model. Hence, numerical diffusion is slightly reduced compared to the previous discretization scheme. However, oscillations appear in the profiles above the thermoclines. The oscillations are increasing as the charging phase continues. This is also mentioned in [55], where the authors noticed spatial oscillations when a sharp gradient was represented with a higher order discretization scheme. Moreover, the computational time is the same for the two discretization schemes. Thus, changing the derivation scheme for centered finite differences does not appear to be a good approach.

In order to eliminate numerical diffusion, Powell *et al.* [41] developed an intermediate model between the ideally stratified model and the multinode model. Two variable volumes represent the hot and the cold zones on each side of the thermocline. The thermocline itself is modeled with a fine 1D grid along the vertical axis. When the charging or discharging begins from a uniform temperature storage tank, the thermocline is created while the fluid crosses the thin

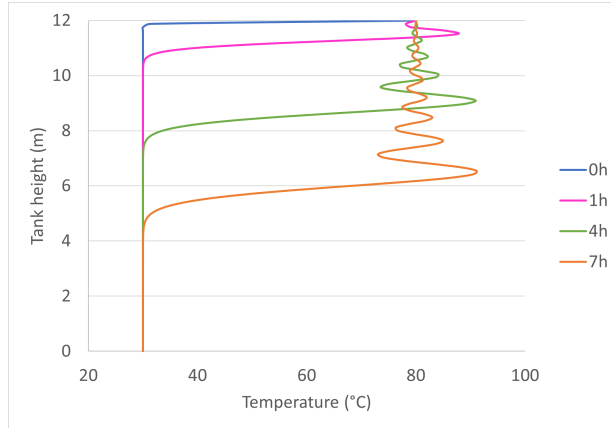


Figure 5: Temperature profiles obtained with centered finite differences and 100 layers

layers of the grid. Once the thermocline is established, it will move up and down the storage tank and only the hot and cold volumes will vary. With this approach, numerical diffusion is eliminated, the model runs faster than the traditional multinode model and does not overestimate the storage capacity as the ideally stratified model does. Thus, this model is accurate and fast enough for dynamic simulations. Unfortunately, conditional structures make it difficult to incorporate into an optimization model.

In this paper, a new discretization scheme is applied to the storage tank vertical axis in order to make numerical diffusion negligible and better represent the storage tank.

4. New spatial discretization scheme

4.1. General presentation of Orthogonal Collocation

Orthogonal Collocation (OC) approximates the unknown state variable involved in a differential equation with a sum of some selected trial functions of the integration variable. In this case, the unknown variable is the temperature inside the storage tank $T(z)$ and the integration variable is the space coordinate z . Equation 11 shows the construction of the approximate temperature $\tilde{T}(z)$ with the trial functions f_i^{trial} :

$$T(z) \approx \tilde{T}(z) = \sum_{i=1}^N a_i f_i^{trial}(z) \quad (11)$$

With this method, the derivative of the temperature can be easily computed with the derivatives of the trial functions, which are known analytically. The satisfaction of the differential equation is imposed for N points carefully chosen and called collocation points. This method allows the transformation of a differential equation into a system of algebraic equations, whose unknowns are the coefficients a_i associated with each trial function in the sum. Generally, polynomials are used as trial functions. Collocation points are commonly chosen as the roots of orthogonal polynomials, hence the name Orthogonal Collocation. The choice of the collocation points will impact the convergence and accuracy of the results. Moreover, orthogonal polynomial roots allow to use a quadrature method in order to compute the integral of the unknown variable. Polynomial interpolation ensures the continuous representation of the variable over the integration domain. On the contrary, finite volumes only provide the values for distinct discretization points. Linear interpolation can then be used to obtain a continuous solution. For the same degree of accuracy, less points are needed and thus less computational time, for OC. For these reasons, Equation 1 was discretized with OC for the space variable z in the next subsections.

4.2. Implementation methodology

To the best of our knowledge, OC has never been applied to discretize the space dimension of a storage tank. This subsection presents the methodology developed. The unknown temperature along the z axis is represented by a linear combination of N interpolating Lagrange polynomials l_j (numbered from $j=1$ to N), which is a common choice for the trial functions of OC. The vertical axis is discretized with N collocation points z_i . The advantage of Lagrange polynomials is the following property: $l_j(z_i) = \delta_{ji}$, which is 1 if $j = i$ and 0 if $j \neq i$. Thus, the temperature can be written as follows:

$$T(z) \approx \tilde{T}(z) = \sum_{i=1}^N T_i l_i(z) \quad (12)$$

The characteristics of Lagrange polynomials allow us to write: $T(z_i) = T_i$ for the temperature at each collocation point i . Thus, the coefficients involved in the linear combination used to approximate the temperature along the z axis are the temperatures in each collocation point. Diverse matrices formulations were developed for OC. An advantage of the matrix methods is that the matrices used to express the differential terms only depend on the collocation points. Therefore, once the points are chosen, the matrices can be computed once and then used in all the simulations and optimizations. That way, their construction does not participate in the computational time. One formulation takes advantage of the properties of Lagrange polynomials to build an accurate matrix method [56]. Ebrahimzadeh *et al.* [57] detailed the following steps for the implementation of this method, here applied to the discretization of the height of the storage tank:

1. Normalise the domain (the height of the storage tank) between 0 et 1 :

$$z^* = \frac{z}{H}$$
2. Choose N_{int} interior collocation points as roots of orthogonal polynomials. Shift then in $[0,1]$ if necessary. The complete set of collocation points is composed of the N_{int} points and the boundary points 0 and 1
3. The interpolation polynomial representing the temperature along the z axis is passing through the $N_{int} + 2$ collocation points and has a degree of $N_{int} + 1$. It can be written as a linear combination of $N_{int} + 2$ Lagrange polynomials passing through the $N_{int} + 2$ collocation points:

$$T(z) \approx T_{N_{int}+1}(z) = \sum_{i=1}^{N_{int}+2} T_i l_i(z) \quad (13)$$

4. The interpolation polynomial can then be differentiated by using the expression of the derivatives of Lagrange polynomials:

$$\frac{\partial T(z)}{\partial z} \approx \frac{\partial T_{N_{int}+1}(z)}{\partial z} = \frac{1}{H} \sum_{i=1}^{N_{int}+2} \frac{\partial l_i(z)}{\partial z} T_i \quad (14)$$

This Equation can be written for each collocation point, and the system can be put in matrix form: $dT = A_{OC}T$. The coefficients in matrix A_{OC}

are $A_{OCij} = \frac{dl_j(z_i)}{dz}$ for i and j varying from 1 to $N_{int} + 2$ and T is a column vector containing all the T_i values. dT is a column vector containing all the dT_i values, which are the first derivatives of the temperature with respect to z for each collocation point i , and are expressed as a linear combination of the temperatures T_i .

5. The same method can be applied to the second derivative, with a matrix B_{OC} and a column vector d^2T containing the second derivatives d^2T_i of the temperature with respect to z for each collocation point i . If the domain has been normalized, we have $\frac{\partial T(z)}{\partial z} = \frac{1}{H} \frac{\partial T(z^*)}{\partial z^*}$, and similarly, $\frac{\partial^2 T(z)}{\partial z^2} = \frac{1}{H^2} \frac{\partial^2 T(z^*)}{\partial z^{*2}}$.
6. The differential terms in Equation 1 can then be replaced by $\frac{A_{OC}T}{H}$ and $\frac{B_{OC}T}{H^2}$. This forms a system of N_{int} equations with $N_{int} + 2$ unknowns which are the temperatures at each collocation point. Two boundary conditions complete the system (see subsection 4.3)

With OC, Equation 1 is transformed into a system of ODEs and the time integration is performed in MATLAB with the solver ode15s. The ODE equations are written as follows for each interior collocation point i :

$$\rho C_p A \frac{dT_i}{dt} = UP(T_{amb} - T_i) + k^* A \frac{d^2 T_i}{H^2} - (\dot{m}_c - \dot{m}_d) C_p \frac{dT_i}{H} \quad (15)$$

The time dependency of the variables in this equation is not written for conciseness. The boundary conditions are those defined in Section 2 and a new formulation able to adapt to the working mode of the storage tank is presented in 4.3.

The collocation points associated with Gauss-Lobatto quadrature are chosen. This will allow an accurate calculation of the stored energy inside the storage tank, which requires the integration of the temperature profile over the height of the tank. For an interpolation polynomial of degree $N_{int} + 1$, the collocation points are the two boundary points of the interval and the roots of the derivative of the orthogonal polynomial of degree $N_{int} + 1$. In the simulations, the roots of Chebyshev polynomials were chosen as collocation points. They were found to perform better than Legendre polynomials.

4.3. Boundary Conditions

As mentioned in subsection 4.2, to use OC with N collocation points ($N = N_{int} + 2$) for the discretization of the space coordinate in the storage tank, two boundary conditions are needed in addition to the energy balance written for the interior collocation points. In this case, Equation 1 has a second derivative term for the space variable, therefore two boundary conditions are required: one at the bottom of the tank (point 1, $z = 0$) and one at the top (point N , $z = H$). For finite volumes discretization, the energy balance was written for the top and bottom layers, assuming that the derivative of the temperature with respect to space was zero at the boundary. With OC, no energy balance is written for the boundary points, and boundary conditions are directly added to the system of differential equations. The boundary conditions, which depend on the working mode of the storage tank, were presented in Section 2. In the simulation or the optimization of an energy system including a storage tank, the model needs to switch to the appropriate boundary conditions automatically. Conditional structures would slow down the convergence of the calculations and should be avoided. In the multinode model, the energy balance written for the top and bottom layer involve the flow rates of charge and discharge. Thus, it is able to represent all the working modes. The idea detailed hereafter is to apply an energy balance on a small layer of fluid located at the top and at the bottom of the tank in order to compute the boundary temperatures. This is similar to the mixing zones mentioned in [28]. Pate also wrote an energy balance at the boundary points but neglected the accumulation term [24]. This formulation did not require the construction of a small layer of fluid and was solved locally. However, since the inertia was neglected, it was found to generate oscillations in the boundary temperatures. Thus, mixing zones were preferred.

The boundary condition at the bottom of the tank, $z = 0$, is written as follows:

$$\rho C_p A \Delta z \frac{dT_1}{dt} = U_1 S_1 (T_{amb} - T_1) + \frac{4}{3} \frac{k^* A}{\Delta z} (T_2 - T_1) + \dot{m}_c C_p (T_2 - T_1) + \dot{m}_d C_p (T_{return} - T_1) \quad (16)$$

T_1 represents the temperature of the boundary and T_2 is the temperature of the first interior collocation point.

The boundary condition at the top of the tank, $z = H$, is written as follows:

$$\rho C_p A \Delta z \frac{dT_N}{dt} = U_N S_N (T_{amb} - T_N) + \frac{4 k^* A}{3 \Delta z} (T_{N-1} - T_N) + \dot{m}_c C_p (T_{charge} - T_N) + \dot{m}_d C_p (T_{N-1} - T_N) \quad (17)$$

T_N represents the temperature of the boundary and T_{N-1} is the temperature of the last interior collocation point. The time dependency of the variables in these equations is not written for conciseness. The impact of the thickness Δz of this mixing zone was assessed. It appeared that using the distance between the boundary point and the closest collocation point as the layer thickness was appropriate. The temperature profiles obtained during the charging phase were in total agreement with the ones obtained with fixed boundary conditions corresponding to a charge. The computational times were also similar. When the fixed boundary conditions are used, the temperature at the top of the storage tank is the temperature of the charged fluid. However, with the mixing zone, an energy balance is used, so the temperature is not immediately equal to the charging temperature. Figure 6 shows the variations of temperature at the top point during the charging of the storage tank for fixed boundary conditions and mixing zones. The temperature at the very beginning of the simulation is not included in Figure 6 for the mixing zone because it is much smaller than the charging temperature. During the first time instants, there is some mixing between the charged fluid and the stored fluid, which seems realistic. We observe that the top temperature quickly reaches the charging temperature and slightly oscillates around it during the first hours. However, these oscillations are small, less than 0.4°C . The model with mixing zones to represent the changing boundary conditions is therefore validated.

4.4. Importance of the diffusion term

In some studies, the diffusion term in Equation 1, $Ak \frac{\partial^2 T(z,t)}{\partial z^2}$, is neglected ([26],[33], [44], [47]). Nevertheless, He *et al.* [11] showed in an experimental

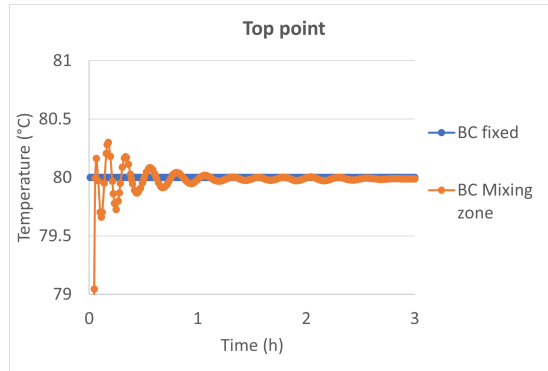


Figure 6: Temperature evolution at the top of the tank during charging

study the expansion of the thermocline during the stand-by status. They highlighted the importance of reducing the duration of those idle periods in order to preserve the quality of the stored energy. First, the impact of the diffusion term during the idle periods was assessed in a simulation in MATLAB. A stand-by period of 48 hours was considered, which corresponds to a long idle period for a daily storage tank. Heat losses to the environment are included in the model. The storage tank is initially half charged and the vertical axis is discretized with 200 collocation points. Two simulations are run, one considering the diffusion term and the other neglecting it.

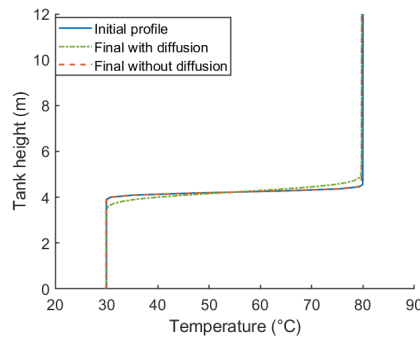


Figure 7: Effect of the diffusion term during idle periods

Figure 7 presents the initial and final profiles with and without the diffusion term. First, we can notice that the hot temperature in the tank decreases

slightly due to heat losses for the two simulations. When diffusion is considered, the thermocline thickens over time, but the effect is rather small. The computational times for these two simulations are similar (0.12s without diffusion and 0.15s with diffusion). A quantitative comparison of the stored energy inside the tank was performed. Here, the energy is valuable above 65°C. The initial valuable energy stored is 18.54MWh. After 48 hours, this value is 18.45MWh when diffusion is neglected, which represents a drop of 0.49% due to heat losses. When the diffusion is modeled, the valuable stored energy after 48 hours is 18.23MWh, which is a decrease of 1.67% compared to the initial state. Thus, in this model, diffusion does lead to a slight destratification but the effect is small. Experimental studies showed a larger impact of diffusion on energy degradation [11]. Other effects than diffusion can lead to some mixing. For instance, the heat losses are larger along the tank walls. The fluid close to the walls is cooled down and sinks along the wall, generating convection movement that mixes the stored fluid. Diffusion is probably negligible compared to these convection movements and the destratification is mostly due to these 3D convection movements. Unfortunately these 3D phenomena are difficult to model in 1D.

So these simulations showed that the diffusion term does not have a great impact on the temperature profiles inside the storage tank during idle periods. A second test has been conducted to assess the importance of the diffusion term during charging or discharging. Figure 8 shows the temperature profiles in the tank at 4 time instants during the charging phase of the storage tank for the models neglecting or not the diffusion term. It can be observed that oscillations appear on each side of the thermocline region when diffusion is neglected. Therefore, it is a good practice to keep the diffusion term when discretizing the storage tank with orthogonal collocation. This term has a stabilizing behavior.

5. Orthogonal Collocation: results and discussion

The methodology explained in the previous section was applied to discretize the vertical axis of the storage tank during a simulation of a charging phase.

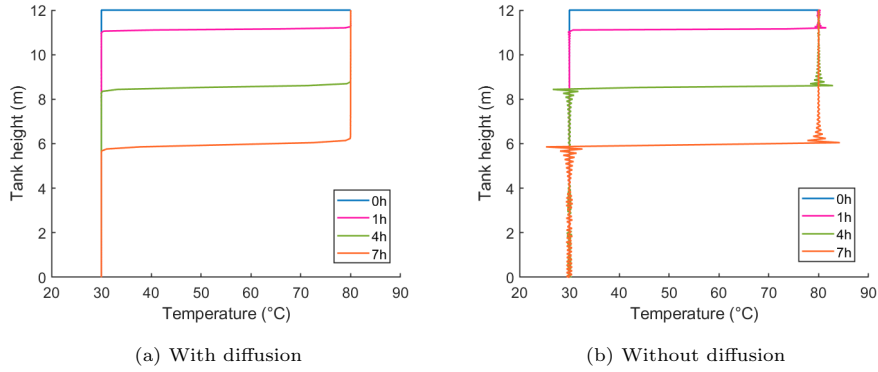
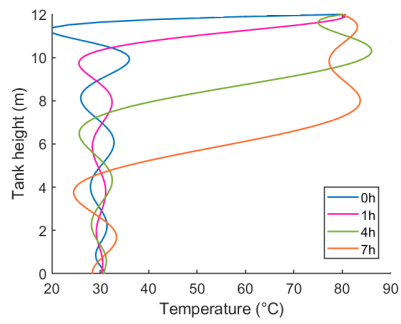


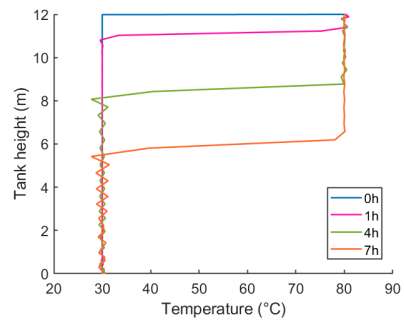
Figure 8: Effect of the diffusion term during the charging phase

The storage tank is initially at a uniform temperature of 30°C and is charged with a hot fluid at 80°C with a flow rate of $10\text{kg}\cdot\text{s}^{-1}$. A sensitivity analysis on the number of collocation points is conducted to assess its effect on the temperature profiles. Figure 9 shows the temperature profiles at 4 times instants during a charging phase, with 10, 50, 100, 150 collocation points, along with the computational times required to perform the 26 hours charge. Firstly, it can be observed that the temperature profiles with a model with few collocation points are not smooth and present oscillations in the temperature, especially around the thermocline region. These oscillations fade away when the number of points is increased. It can be noticed that the slope of the thermoclines is correctly estimated with only 50 points. As expected, the computational time increases with the number of points but they stay reasonable for simulations.

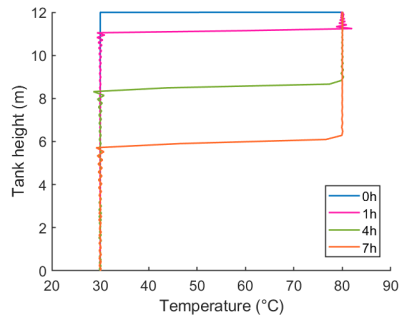
The impact of the number of points on the valuable stored energy over time was also assessed. Figure 10 represents the cumulated stored energy at a temperature above 65°C for different numbers of collocation points. It can be observed that the energy computed with the model with 10 points differs from the other energy profiles. For 50 and 200 collocation points, the energy profiles are the same. This shows that the oscillations in the temperature profiles do not impact the stored energy estimation. The oscillations probably compensate along the temperature profile. However, the thermocline slope needs to be accurately



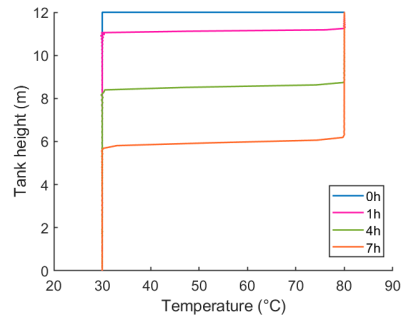
(a) 10 points: 0.11s



(b) 50 points: 0.26s



(c) 100 points: 0.44s



(d) 150 points: 0.90s

Figure 9: Impact of the number of collocation points on the temperature profiles

represented in order to estimate correctly the stored energy. A quantitative analysis was performed. The maximal difference between the energy computed with the 200 points model and the 10 points model is 1.1MWh and for the 50 points model it is 0.14MWh. The maximal relative difference is reached at the beginning of the charging phase when the energy is small. It is 27% for the 10 points model and 2.8% for the 50 points model compared to the 200 points model.

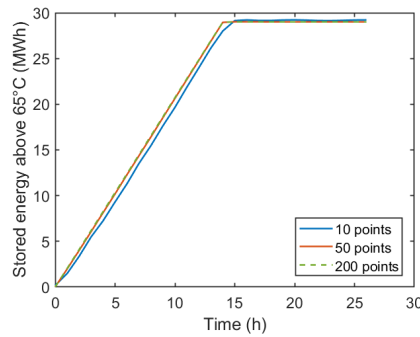


Figure 10: Cumulated stored energy throughout time during charging

The results obtained are compared with the multinode model (see subsection 3.2). The chosen reference is OC with 200 collocation points because the results converge towards the same solution with a larger number of collocation points. The multinode model with 1000 layers underestimates the stored energy by up to 0.46MWh, and up to 8% at the beginning of charge. The difference is small but still more important than the difference between the stored energy with 50 points with OC and 200 points. This confirms that OC gives a better estimation of the temperature gradient, despite some oscillations around the thermocline, which do not impact the stored energy much. With 5000 layers in the multinode model, the relative difference with the reference is 2.9% and the absolute difference is 0.16MWh. These differences are similar to the ones observed with 50 collocation points. In terms of temperature profiles, 5000 layers in the multinode model and 200 collocation points lead to similar results, plotted in Figure 11. In this figure, a temperature profile is plotted every hour

until the charge is complete, with solid black line for OC with 200 collocation points and dashed red lines for the multinode model with 5000 layers. Both models give similar results, although the multinode model still presents slight numerical diffusion. The largest difference between the temperatures from the two models at the same height is 5.9°C , and the maximal relative difference is 17%. These differences are not negligible but even more layers would be necessary in the multinode model in order to find the same results as OC. The computational times are very different: 0.85s for OC and 330s for multinode. This clearly shows the advantage of using OC over finite volumes to discretize the storage tank.

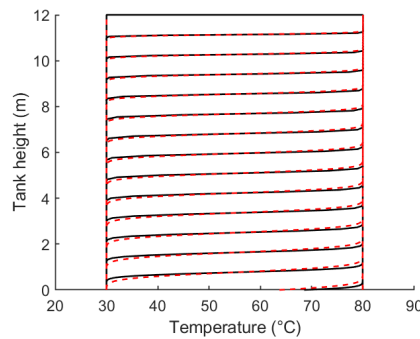


Figure 11: Comparison of the temperature profiles throughout time with 200 collocation points (solid black lines) and 5000 layers (dashed red lines)

This study showed that OC greatly reduces numerical diffusion and is able to accurately represent the steep temperature gradient in the thermocline region even with a small number of collocation points. However, oscillations appeared in the spatial temperature profiles around the thermocline for a smaller number of collocation points. The reason for these oscillations is that a low-degree polynomial is not able to represent a very steep gradient. By increasing the number of collocation points, hence the degree of the temperature polynomial, the oscillations fade away.

For a simulation model, OC with 100 to 200 collocation points seems to provide accurate and fast results. Thus, the problem of oscillations will not

arise because the number of collocation points is large enough. However, for an optimization model, computational times might be too long. The number of points should probably be reduced. The next section will introduce Orthogonal Collocation on Finite Elements (OCFE), which present some advantages over OC and might be more suited for an optimization study.

6. Orthogonal Collocation on Finite Elements

When the discretization domain is large or when an important number of collocation points is required, Orthogonal Collocation on Finite Elements (OCFE) is generally more appropriate [58]. The domain is divided into elements and OC is applied in each element. The continuity of the differential variable and its first derivative (in the case of a 2^{nd} order differential equation) is imposed at the boundaries between elements. This method gathers the advantages of the two previously mentioned discretization techniques. The convergence is fast, as in OC, which allows to use a smaller number of discretization points. The resolution is fast as for the finite volumes method. OCFE involves sparse matrices, while OC involves full matrices. Thus, OCFE is faster to solve than OC. Carey and Finlayson recommend using OCFE when there is a zone with a steep gradient in the solution, by adapting the size and position of the elements to the expected solution [58]. For example, OCFE is particularly well suited to model boundary layers. In the storage tank, there is indeed a zone with a steep gradient, the thermocline. Unfortunately, its position moves inside the storage tank. It is therefore not possible to use fixed smaller elements around the thermocline. Moving elements could be a good direction for future works but it is more complex to implement in an optimization study than fixed elements.

Yet, OCFE presents promising advantages over OC, such as its fast resolution. Therefore, it might be more appropriate than OC for optimization studies. In order to assess OCFE performances for optimization studies, a simulation model for the storage tank was built in an optimization environment. The software GAMS was used and the model was solved with the optimization

solver IPOPT. The simulation model developed can be directly incorporated into an optimization model in GAMS. The model is built similarly to the OC model explained in 4.2. The energy balance can be written for each interior point i of each element j . This is represented by the following equation:

$$\rho C_p A \frac{dT_{j,i}}{dt} = UP(T_{amb} - T_{j,i}) + k^* A \frac{d^2 T_{j,i}}{L_{el}^2} - (\dot{m}_c - \dot{m}_d) C_p \frac{dT_{j,i}}{L_{el}} \quad (18)$$

The time dependency of the variables in this equation is not written for conciseness. The first and second derivatives of the temperature with respect to z , $dT_{j,i}$ and $d^2 T_{j,i}$ respectively, are expressed as a linear combination of all the temperatures $T_{j,i}$ in the collocation points of the corresponding element. The matrices A_{OCFE} and B_{OCFE} , computed with the Lagrange polynomials derivatives evaluated in each collocation point inside an element, as explained in 4.2, are used to express the linear combination. L_{el} is the length of each element. We consider N the total number of collocation points in each element. The continuity equations between elements for the temperature and its first derivative with respect to time are written as follows:

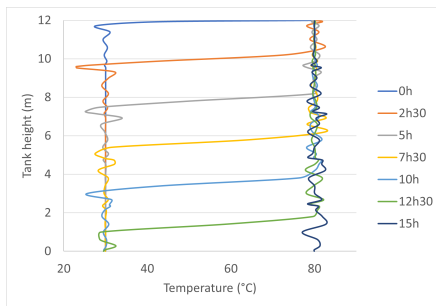
$$T_{j-1,N} = T_{j,1} \quad (19)$$

$$\frac{dT_{j-1,N}}{dt} = \frac{dT_{j,1}}{dt} \quad (20)$$

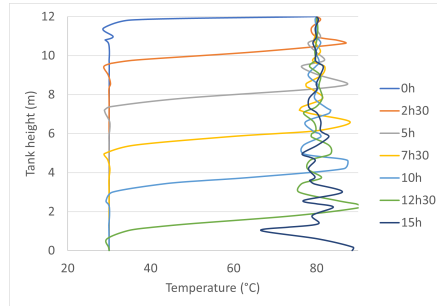
One major difference between MATLAB and GAMS is the time integration. In MATLAB, the simulation model was solved with the solver `ode15s`, using a variable time step. In GAMS, the time discretization must be explicitly written by the user. We chose orthogonal collocation on finite elements for the time discretization. The time step does not adapt to the simulation but is fixed in advance. Elements of 15 minutes are chosen, with 5 collocation points in each element, including the boundary points. The collocation points are the Gauss-Lobatto Legendre points. The matrix method implemented for the time discretization is based on [59] and detailed in [53]. This method is particularly suited for initial value differential equations. The length of the time elements needs to be chosen carefully to respect the convergence criteria even though the

spatial grid is non-uniform. Indeed, numerical instabilities might arise if the time step is too large compared to the space discretization [53]. Generally, it is recommended to ensure that the fluid does not flow through several space discretization points during a single time step. Of course, with OCFE, both time and space discretization are non-uniform. It is necessary to ensure that the recommendation is followed for every time and space steps. This is only a general recommendation and a time step 2 or 3 times larger might not generate numerical instabilities. OC was used to discretize the vertical axis of the storage tank to provide a comparison in this study. Figure 12 shows the temperature profiles obtained during a charging phase for OC and OCFE with the same total number of points, along with the computational times for the complete charge. This figure shows that OC is the most accurate but its resolution takes the longest. OCFE results depend on the number of elements and points. The more elements are used for the same total number of points, the less accurate the solution is. That is expected because the energy balance in Equation 1 is only performed on the interior points. At the boundary points between elements, continuity equations are derived. Based on these results, it is recommended to use OCFE in an optimization code because it is much faster to solve. However, a sufficient number of collocation points should be used in each element to ensure a good accuracy in the results.

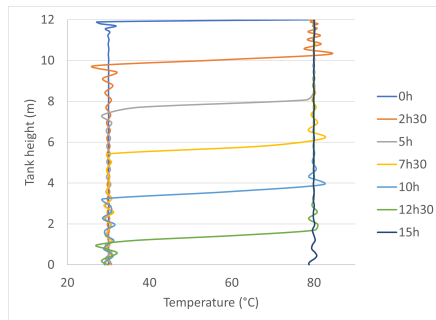
Unfortunately, a very large number of elements or collocation points can not be used in an optimization study because it would increase the computational time too much. Thus, oscillations in the temperature profiles will not be avoided by increasing the number of points (see Section 5). These oscillations are due to the representation of very thin thermoclines with polynomials. The steepness of the temperature gradient in the thermocline is actually unknown. A validation with a real system will be conducted in Section 7. It is possible that the thermocline representation obtained with the accurate resolution of Equation 1 for a charging phase starting with a uniform storage tank is too steep and not realistic. The next study conducted was the assessment of the performances of OCFE when the initial condition of the storage tank is not a uniform temper-



(a) 5 elements, 10 points (10 s)



(b) 10 elements, 5 points (7 s)



(c) 50 points (34 s)

Figure 12

ature, but rather a thermocline. This initial condition is more likely to happen in an energy system, since it is avoided to completely empty or fill up a storage tank in a real system. This strategy is used because the beginning of charging is when the thermocline thickens the most [11]. It is then better to create the thermocline carefully, by using a small flow rate for example, and then try to keep it inside the storage tank. For this calculation, OCFE was used and the charging phase was simulated in GAMS in anticipation for future optimization studies using this software. The solver IPOPT was used. As mentioned above, it is much faster to use OCFE in GAMS than OC for the same total number of collocation points. In the simulations performed, an initial thermocline exists in the middle of the storage tank. The charging phase starts, with a flow rate of $10\text{kg}\cdot\text{s}^{-1}$ and a temperature equal to the hot section of the storage. Two cases were tested: a multinode model with 500 layers and an OCFE model with 5 elements and 10 collocation points each. The results are plotted in Figure 13. Firstly, there are no major oscillations visible in the OCFE temperature profiles even though only 50 discretization points were used. This is because the initial thermocline is not too steep and therefore, a low degree polynomial representation can approximate it accurately. Moreover, a slight numerical diffusion can be observed for the multinode temperature profiles. The thermocline thickens slightly during the charging phase. On the other hand, the thermocline thickness remains unchanged with OCFE. Therefore, OCFE was able to greatly reduce numerical diffusion. Finally, the computational times are very different: 7s for OCFE and 1000s for the multinode model to complete the charge of the storage tank.

We showed that a small number of collocation points is able to accurately represent the temperature profiles in the tank when the thermocline is already created. OCFE runs much faster than the multinode model to achieve comparable accuracy.

In this section, the results obtained with the multinode model and OC/OCFE were compared. With a sufficiently large number of discretization points, a convergence in the results is achieved. Therefore, we have access to the solution of

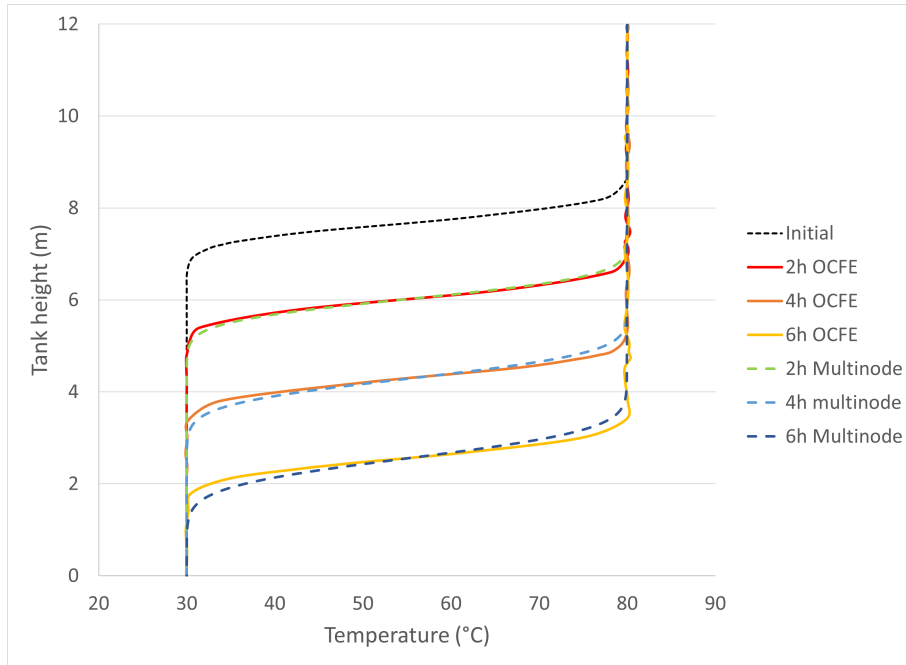


Figure 13: Comparison of the temperature profiles for the multinode model and OCFE during a charging phase from a half charged tank

Equation 1. We showed that OC performs better than the multinode model in order to solve this equation accurately and rapidly. However, Equation 1 might not be an accurate representation of the reality. Therefore, the next section will present a validation of our OCFE model with real plant data.

7. Validation with a real system

7.1. Condat-Sur-Vézère, France, Solar Thermal Plant

NEWHEAT is a French company specialized in solar thermal plants, taking part in each stage of their life: design, financing, building and operation. Their solar thermal plants are providing heat at a competitive price to industrial processes or district heating networks. In June 2019, NEWHEAT inaugurated a solar thermal plant in Condat-Sur-Vézère, in the South-West of France. At the time, it was the largest solar thermal plants with flat plate collectors in

France and the first in the world to use a 1-axis solar tracking system. The heat produced by this plant is delivered to a paper mill. A water storage tank of $450m^3$, with a height of 11.25m, allows the decoupling between the heat production and consumption. The solar plant has been instrumented for accurate measurements of flow rates and temperatures. Especially, 11 thermocouples are measuring the temperatures along the vertical axis of the storage tank. The flow rates and temperatures for the charging and return flows are also measured. It was therefore possible to use real plant data to validate our storage tank model.

7.2. Validation

In order to validate the OCFE model presented above, a simulation is performed over a charging cycle and compared to real plant data. The initial temperatures inside the storage tank at the beginning of the charging phase, as well as the charging flow rate and temperature are used as inputs to the simulation model. The data were acquired on June 3rd, 2019, with a time resolution of 10 minutes. The charging phase begins at 2pm. The multinode model as well as the OCFE model presented in Section 6 were compared to the experimental data. The simulations were performed in GAMS with the IPOPT solver. For the multinode model, a simplified simulation with 10 layers was first conducted. The time discretization uses elements of 1 hour and 9 collocation points. The results are plotted in Figure 14a, and the charging phase simulation lasted 2 seconds. The temperature profiles at 3pm, 6pm and 9pm for the experimental data and for the model are plotted. The uncertainty in the temperature measurement is ± 0.5 °C, which is too low to be represented on the plot. We observe that numerical diffusion has an important impact on the numerical temperature profiles and that there is a poor agreement between the experimental and modeled values. Another simulation with 100 layers was then run, with a finer time discretization. Elements of 30 minutes were used in order to avoid numerical instabilities due to the smaller space elements. The results are presented in Figure 14b. The effect of numerical diffusion is less visible in this plot. A better agreement is noticed between the experimental and modeled

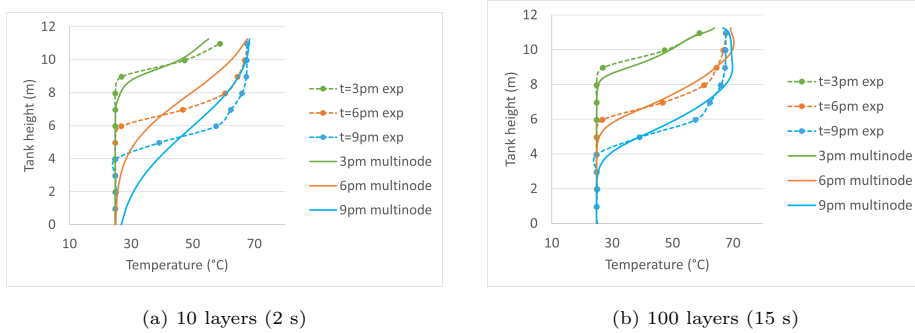


Figure 14: Comparison of the experimental and multinode model temperature profiles during a charging phase

temperature profiles. However, the simulation lasted 15 seconds, which is 7 times longer than the simulation with 10 layers. For this simple system, with only the storage tank, and a short time horizon, the computational times are short in both cases. Nevertheless, for the simulation of a more complex system including storage or for an optimization study, the computational time might become too long with 100 layers. This is even more important for real-time optimization.

The OCFE model developed in this paper was then compared to the experimental results. The model in GAMS validated for optimization studies uses 3 elements and 8 collocation points. The time discretization uses elements of 1 hour and 9 collocation points, which is the same as the multinode model with 10 layers. The results are plotted in Figure 15, and the computational time for the charging phase is 3 seconds. This is very close to the computational time for the multinode model with 10 layers, and 5 times faster than the model with 100 layers. Moreover, as shown in Figure 15, the thermoclines are here well represented. There is a good agreement between the numerical and experimental profiles.

The error made by the models was quantified with two indicators: Mean Absolute Error (MAE) and Mean Absolute Percentage Error (MAPE). These

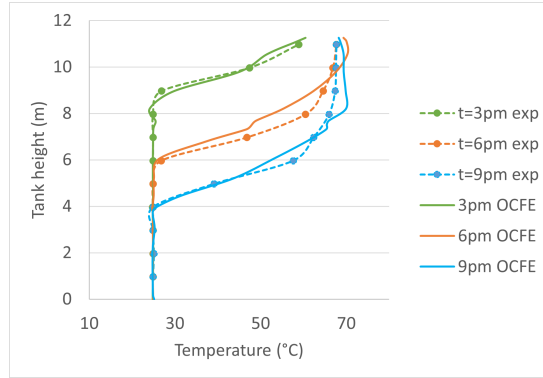


Figure 15: Comparison of the experimental and OCFE model temperature profiles during a charging phase

Time	10 layers			100 layers			3x8 OCFE		
	3pm	6pm	9pm	3pm	6pm	9pm	3pm	6pm	9pm
MAE (°C)	1.1	4.4	5.3	1.1	1.6	1.9	0.7	1.9	1.5
MAPE (%)	3.1	11.5	15.9	3.5	3.7	4.2	1.8	3.8	2.8

Table 1: Validation of the numerical models

are defined as follows:

$$MAE(^{\circ}C) = \frac{1}{k} \sum_{i=1}^k |x_i - y_i| \quad (21)$$

$$MAPE(\%) = \frac{1}{k} \sum_{i=1}^k \left| \frac{x_i - y_i}{x_i} \right| \quad (22)$$

In these Equations, k is the number of comparison points, x_i are the experimental points and y_i are the numerical points. To ensure that x_i and y_i are taken at the same height in the storage tank, the numerical profile obtained is interpolated. The results for these two indicators are presented in Table 1 for the three models tested.

Table 1, confirms that the model with 10 layers is not accurate with MAPE going up to 15.9%. The two other models have a MAPE below 5% for 100 layers and 4% for OCFE. The MAE is below 2°C, which is small compared to

the accuracy of the temperature measurements. Therefore, these models are considered valid. With OCFE, we were able to use less points and achieve a better accuracy than the multinode model. Thus, the OCFE model presented in this study is validated and should be used to discretize a TES for simulation and optimization studies.

This validation study was conducted for a charge cycle, starting once the thermocline inside the storage tank is created. The beginning of charge from an empty storage is not well represented by Equation 1. Indeed, there is some mixing happening when the fluid enters the storage tank, leading to a thicker thermocline than the one predicted by the model. Developing diffusers that prevent this effect is still an active area of research ([60], [61] for example). To accurately represent this phenomenon in a 1D model, data reconciliation should be performed and an additional diffusion term should be introduced in the model to account for the mixing due to injection. This has been done for reactors modeling to represent non-ideal flow patterns [62]. This would require a large amount of data with a fine spatial and temporal resolution. In real applications, it is avoided to completely empty or fill up the storage tank. Therefore, the model presented in this paper is accurate to represent the real conditions inside the storage tank.

8. Perspectives on natural convection modeling

As mentioned in Section 2, the correction of temperature inversions inside the storage tank is an important aspect of TES modeling. It is particularly challenging to incorporate natural convection in a 1D model appropriate for optimization studies. Indeed, a continuous and smooth model is required for optimization. Such a model was developed based on the physical model suggested in [28]. A turbulent diffusion coefficient was added to correct the temperature inversions, and had the following value:

$$\epsilon_{turb} = \frac{k_{turb}}{\rho C_p} = \begin{cases} (K\delta l)^2 \sqrt{g\beta \frac{\partial T(z,t)}{\partial z}}, & \text{if } \frac{\partial T(z,t)}{\partial z} < 0 \\ 0, & \text{otherwise.} \end{cases} \quad (23)$$

In this Equation, K is the Von Karman constant, whose value is 0.4, g is the gravitational acceleration which is 9.81 m.s^{-2} and β is the thermal expansion coefficient of water, which is about $2.6e^{-4} \text{ K}^{-1}$. The characteristic length δl is chosen to be the tank height.

Such inversions correspond to a reversed temperature gradient. With z axis pointing upwards, the gradient in normal conditions is positive, and in case of temperature inversion it is negative. It is thus possible to spot a temperature inversion thanks to the max function, with the turbulent coefficient written as:

$$k_{turb} = \rho C_p (KH)^2 \sqrt{g\beta \mathbf{max}\left(-\frac{\partial T(z,t)}{\partial z}, 0\right)} \quad (24)$$

This formulation can be incorporated into an OCFE model for TES simulation. The boundary conditions used are presented in Subsection 4.3. 100 collocation points are used in this study. Figure 16 presents the results of a simulation with an inversion correction. In this study, the hot zone of the storage tank is initially at 80°C . The storage tank is charged during 1h with fluid at 75°C , and then the charging fluid goes back to 80°C and the simulation runs for 5 more minutes. With this model, the temperature inversion persists as long as the charging with fluid at 75°C is still in progress, as shown in Figure 16. However, after the charging temperature goes back to 80°C , temperature inversions are corrected. The inlet of the storage tank is at 80°C while the rest of the hot zone is at a homogeneous temperature resulting from the mixing between the fluid already present at 80°C and the charged fluid at 75°C . This behavior seems realistic, but the model is much slower than a model without natural convection, about 150 times slower. Unfortunately, no validation with real plant data could be conducted for the natural convection modeling. This would require data from thermocouples that are close to each other and with a small time resolution. Such data were not available in the plant used for the

validation.

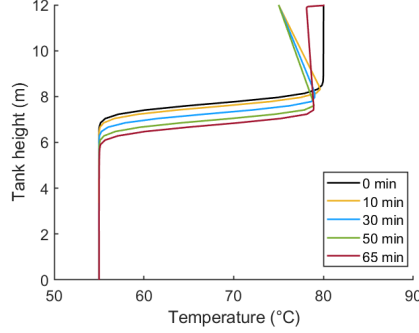


Figure 16: Correction of temperature inversions with a continuous model

For a simulation model, this works fine with the max function, although it is much slower than a model without the inversion correction. For an optimization model, a smooth approximation of the max function needs to be used, such as in [51] and [52]. The parameter determining the steepness of the max function needs to be adjusted to offer a compromise between the accurate representation of the max function and the ease of convergence. This will slow down even more the calculations. For example, the following approximation was used to determine the maximum between two values x_1 and x_2 :

$$\text{smoothMax}(x_1, x_2, d) = 0.5(x_1 + x_2 + \sqrt{(x_1 - x_2)^2 + d^2}) \quad (25)$$

In this formulation, parameter d needs to be adjusted to adapt the steepness of the function. If d is large, the function varies smoothly and temperature inversions are not spotted accurately. This leads to the thickening of the thermocline due to a large diffusion coefficient, even when it is not needed. On the contrary, if d is small, the approximate function better represents the max function and the computation of k_{turb} is more accurate. However, convergence is not ensured.

Figure 17 shows the results obtained with $d = 1e^{-4}$. The results are slightly different from the ones obtained in Figure 16, with a maximum difference of 2.5% in the final profiles. We notice that the average temperature in the hot zone after the correction of the temperature inversion is about 1°C lower with

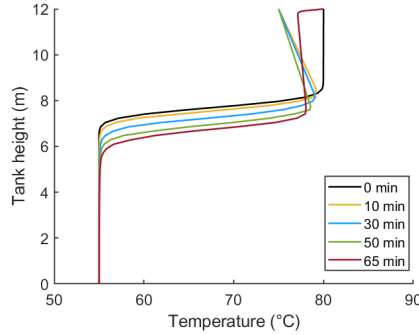


Figure 17: Correction of temperature inversions with a smooth model

the smooth function. This happens because the turbulent coefficient is not 0 in the thermocline region, even though the temperature gradient is not reversed. Thus, there is a large diffusion at the ends of the thermocline, introducing some mixing between colder fluid from the thermocline and hot fluid in the hot zone. Overall the results are in good agreement with the ones obtained with the discontinuous max function. The computational time is about 32 times longer than the model with the max function. If parameter d is smaller, the simulations do not converge.

To conclude, it is possible to build a continuous and smooth model to represent natural convection inside a storage tank. However, this model needs some tuning in the smooth function. The physical basis of the model is therefore deteriorated by these tuning parts. Moreover, the computational time is largely increased when using this model. Based on these observations, it is recommended to choose another solution for the modeling of natural convection in an optimization model. For example, the inversion flow rates presented in [53] appear to be a good solution to correct temperature inversions in an optimization framework. An experimental study should be conducted to validate this model.

9. Conclusion and perspectives

The increasing share of intermittent renewable energies into the electricity grid or heating and cooling district networks requires the development of storage

solutions to ensure that the energy demand is met. Thermal Energy Storage (TES) is an effective way to store energy in the form of heat, that can be latter used, employing the synergies between various energy carriers. In order to expand the use of stratified TES in energy systems, a good model for it needs to be developed. Especially, a fast and accurate model, that can be used for complex dynamic simulations and optimizations is required. A short computational time is even more crucial for real-time optimization and control. The challenge in modeling a thermocline TES is the representation of the steep temperature gradient between the hot and cold zones. The discretization scheme presented in this paper, Orthogonal Collocation on Finite Elements (OCFE), is able to reduce numerical diffusion and therefore estimates accurately the temperature profile inside the tank as well as the valuable energy stored. This model uses less discretization points and runs faster than the multinode model in order to achieve the same accuracy. This discretization method can generate oscillations in the temperature profiles if the storage is initially at a uniforme temperature. The thermoclines estimations are too steep, and thus a low degree polynomial is not able to represent them. Adding a term in the energy balance inside the tank to represent the mixing at the injection point could solve the problem. However, in a real plant, the storage tank is very rarely at a uniform temperature. Therefore, the model presented in the paper is appropriate to represent the actual behavior of a storage tank. This has been validated with real plant data. Thus, the model developed in this work can be used in simulation and optimization, including real-time applications. Finally, a continuous model for the correction of temperature inversions was presented, based on a turbulent diffusion coefficient. The model was able to correct temperature inversions effectively in a simulation. However, the computational time was greatly increased. Transforming it into a smooth model for optimization is even slower, making it not computationally effective. Other ways to model natural convection, as part of the optimization framework, could be better. Future work should focus on the integration of natural convection in a 1D optimization model. Furthermore, the validation of the correction of temperature inversion should be performed with

an experimental set up or a real plant.

Acknowledgements

The project leading to this publication has received funding from Excellence Initiative of Université de Pau et des Pays de l'Adour – I-Site E2S UPPA, a French “Investissements d’Avenir” programme.

References

- [1] Renewable Energy Directive, Directive (EU) 2018/2001 of the European Parliament and of the Council of 11 December 2018 on the promotion of the use of energy from renewable sources, OJ L328/82 (2018).
- [2] M. C. Argyrou, P. Christodoulides, S. A. Kalogirou, Energy storage for electricity generation and related processes: Technologies appraisal and grid scale applications, *Renewable and Sustainable Energy Reviews* 94 (2018) 804–821.
- [3] G. T. Ayele, M. T. Mabrouk, P. Haurant, B. Laumert, B. Lacarrière, Optimal heat and electric power flows in the presence of intermittent renewable source, heat storage and variable grid electricity tariff, *Energy Conversion and Management* 243 (2021) 114430.
- [4] E. Guelpa, V. Verda, Thermal energy storage in district heating and cooling systems: A review, *Applied Energy* 252 (2019) 113474.
- [5] A. Touzo, R. Olives, G. Dejean, D. Pham Minh, M. El Hafi, J.-F. Hoffmann, X. Py, Experimental and numerical analysis of a packed-bed thermal energy storage system designed to recover high temperature waste heat: an industrial scale up, *Journal of Energy Storage* 32 (2020) 101894.
- [6] D. Haillot, E. Franquet, S. Gibout, J.-P. Bédécarrats, Optimization of solar DHW system including PCM media, *Applied Energy* 109 (2013) 470–475.

- [7] S. Ferreira, S. Sochard, S. Serra, F. Marias, J.-M. Reneaume, Modelling of an Adsorption Heat Storage System and Study of Operating and Design Conditions, *Processes* 9 (2021) 1885.
- [8] H. Liang, L. Liu, Z. Zhong, Y. Gan, J.-Y. Wu, J. Niu, Towards idealized thermal stratification in a novel phase change emulsion storage tank, *Applied Energy* 310 (2022) 118526.
- [9] J. Immonen, K. M. Powell, Dynamic optimization with flexible heat integration of a solar parabolic trough collector plant with thermal energy storage used for industrial process heat, *Energy Conversion and Management* 267 (2022) 115921.
- [10] B. Koçak, A. I. Fernandez, H. Paksoy, Review on sensible thermal energy storage for industrial solar applications and sustainability aspects, *Solar Energy* 209 (2020) 135–169.
- [11] Z. He, Y. Qian, C. Xu, L. Yang, X. Du, Static and dynamic thermocline evolution in the water thermocline storage tank, *Energy Procedia* 158 (2019) 4471–4476.
- [12] E. S. ELSihy, Z. Liao, C. Xu, X. Du, Dynamic characteristics of solid packed-bed thermocline tank using molten-salt as a heat transfer fluid, *International Journal of Heat and Mass Transfer* 165 (2021) 120677.
- [13] D. W. Stamps, J. A. Clark, Thermal destratification in a cylindrical packed bed, *International Journal of Heat and Mass Transfer* 35 (1992) 727–737.
- [14] H. Sullivan, K. Hollands, E. Shewen, Thermal destratification in rock beds, *Solar Energy* 33 (1984) 227–229.
- [15] A. Untrau, S. Sochard, F. Marias, J.-M. Reneaume, G. A. Le Roux, S. Serra, Analysis and future perspectives for the application of Dynamic Real-Time Optimization to solar thermal plants: A review, *Solar Energy* 241 (2022) 275–291.

- [16] E. Kleinbach, W. Beckman, S. Klein, Performance study of one-dimensional models for stratified thermal storage tanks, *Solar Energy* 50 (1993) 155–166.
- [17] A. Al-Habaibeh, B. Shakmak, S. Fanshawe, Assessment of a novel technology for a stratified hot water energy storage – The water snake, *Applied Energy* 222 (2018) 189–198.
- [18] Y. Han, R. Wang, Y. Dai, Thermal stratification within the water tank, *Renewable and Sustainable Energy Reviews* 13 (2009) 1014–1026.
- [19] S. M. Hosseinnia, H. Akbari, M. Sorin, Numerical analysis of thermocline evolution during charging phase in a stratified thermal energy storage tank, *Journal of Energy Storage* 40 (2021) 102682.
- [20] S. T. Paing, T. Anderson, R. Nates, Modelling and experimental validation of natural convection heat loss from a solar hot water storage tank, *Asia Pacific - Solar Reaseach Conference* (2019).
- [21] S. Ievers, W. Lin, Numerical simulation of three-dimensional flow dynamics in a hot water storage tank, *Applied Energy* 86 (2009) 2604–2614.
- [22] K. Johannes, G. Fraisse, G. Achard, G. Rusaouën, Comparison of solar water tank storage modelling solutions, *Solar Energy* 79 (2005) 216–218.
- [23] R. De Césaró Oliveski, A. Krenzinger, H. A. Vielmo, Comparison between models for the simulation of hot water storage tanks, *Solar Energy* 75 (2003) 121–134.
- [24] R. A. Pate, A Thermal Energy Storage Tank Model for Solar Heating, thesis, Utah State University, 1977. URL: <https://digitalcommons.usu.edu/etd/7307>. doi:<https://doi.org/10.26076/2a5d-3188>.
- [25] A. Zachár, Analytic solution for convection dominant heat transport induced by buoyant jet entrainment inside hot fluid storage tanks, *Solar Energy* 195 (2020) 239–248.

- [26] A. Campos Celador, M. Odriozola, J. Sala, Implications of the modelling of stratified hot water storage tanks in the simulation of CHP plants, *Energy Conversion and Management* 52 (2011) 3018–3026.
- [27] R. Dickes, A. Desideri, V. Lemort, S. Quoilin, Model reduction for simulating the dynamic behavior of parabolic troughs and a thermocline energy storage in a micro-solar power unit, *Proceedings of ECOS 2015 - The 28th international conference on Efficiency, Cost, Optimization, Simulation and environmental impact of energy systems* (2015) 13.
- [28] M. N. A. Hawlader, T. Y. Bong, T. S. Lee, A Thermally Stratified Solar Water Storage Tank, *International Journal of Solar Energy* 6 (1988) 119–138.
- [29] S. Trevisan, Y. Jemmal, R. Guedez, B. Laumert, Packed bed thermal energy storage: A novel design methodology including quasi-dynamic boundary conditions and techno-economic optimization, *Journal of Energy Storage* 36 (2021) 102441.
- [30] Z. Yang, S. V. Garimella, Molten-salt thermal energy storage in thermoclines under different environmental boundary conditions, *Applied Energy* 87 (2010) 3322–3329.
- [31] A. Mawire, Experimental and simulated thermal stratification evaluation of an oil storage tank subjected to heat losses during charging, *Applied Energy* 108 (2013) 459–465.
- [32] A. Lake, B. Rezaie, Energy and exergy efficiencies assessment for a stratified cold thermal energy storage, *Applied Energy* 220 (2018) 605–615.
- [33] A. Modi, C. D. Pérez-Segarra, Thermocline thermal storage systems for concentrated solar power plants: One-dimensional numerical model and comparative analysis, *Solar Energy* 100 (2014) 84–93.

- [34] A. Rahman, A. D. Smith, N. Fumo, Performance modeling and parametric study of a stratified water thermal storage tank, *Applied Thermal Engineering* 100 (2016) 668–679.
- [35] A. Rahman, A. D. Smith, Predicting heating demand and sizing a stratified thermal storage tank using deep learning algorithms, *Applied Energy* 228 (2018) 108–121.
- [36] T. J. Bird, N. Jain, Dynamic modeling and validation of a micro-combined heat and power system with integrated thermal energy storage, *Applied Energy* 271 (2020) 114955.
- [37] E. Saloux, J. A. Candanedo, Model-based predictive control to minimize primary energy use in a solar district heating system with seasonal thermal energy storage, *Applied Energy* 291 (2021) 116840.
- [38] F. Aguilar, D. Crespí-Llorens, S. Aledo, P. V. Quiles, One-Dimensional Model of a Compact DHW Heat Pump with Experimental Validation, *Energies* 14 (2021) 2991.
- [39] E. Ryan, B. McDaniel, D. Kosanovic, Application of thermal energy storage with electrified heating and cooling in a cold climate, *Applied Energy* 328 (2022) 120147.
- [40] A. Dahash, F. Ochs, A. Tosatto, W. Streicher, Toward efficient numerical modeling and analysis of large-scale thermal energy storage for renewable district heating, *Applied Energy* 279 (2020) 115840.
- [41] K. M. Powell, T. F. Edgar, An adaptive-grid model for dynamic simulation of thermocline thermal energy storage systems, *Energy Conversion and Management* 76 (2013) 865–873.
- [42] S. Scolan, S. Serra, S. Sochard, P. Delmas, J.-M. Reneaume, Dynamic optimization of the operation of a solar thermal plant, *Solar Energy* 198 (2020) 643–657.

- [43] D. Muschick, S. Zlabinger, A. Moser, K. Lichtenegger, M. Göllles, A multi-layer model of stratified thermal storage for MILP-based energy management systems, *Applied Energy* 314 (2022) 118890.
- [44] G. Csordas, A. Brunger, K. Hollands, M. Lightstone, Plume entrainment effects in solar domestic hot water systems employing variable-flow-rate control strategies, *Solar Energy* 49 (1992) 497–505.
- [45] R. Franke, Object-oriented modeling of solar heating systems, *Solar Energy* 60 (1997) 171–180.
- [46] E. M. Kleinbach, Performance Study of One-Dimensional Models for Stratified Thermal Storage Tank, Master’s thesis, University of Wisconsin-Madison, 1990.
- [47] E. Saloux, J. Candanedo, Modelling stratified thermal energy storage tanks using an advanced flowrate distribution of the received flow, *Applied Energy* 241 (2019) 34–45.
- [48] A. L. Nash, A. Badithela, N. Jain, Dynamic modeling of a sensible thermal energy storage tank with an immersed coil heat exchanger under three operation modes, *Applied Energy* 195 (2017) 877–889.
- [49] R. Viskanta, M. Behnia, A. Karalis, Interferometric observations of the temperature structure in water cooled or heated from above, *Advances in Water Resources* 1 (1977) 57–69.
- [50] Y. Zurigat, A. Ghajar, P. Moretti, Stratified thermal storage tank inlet mixing characterization, *Applied Energy* 30 (1988) 99–111.
- [51] J. Lago, F. De Ridder, W. Mazairac, B. De Schutter, A 1-dimensional continuous and smooth model for thermally stratified storage tanks including mixing and buoyancy, *Applied Energy* 248 (2019) 640–655.
- [52] A. Soares, J. Camargo, J. Al-Koussa, J. Diriken, J. Van Bael, J. Lago, Efficient temperature estimation for thermally stratified storage tanks with buoyancy and mixing effects, *Journal of Energy Storage* 50 (2022) 104488.

- [53] S. Scolas, Développement d'un outil de simulation et d'optimisation dynamique d'une centrale solaire thermique., thesis, Pau, 2020. URL: <https://theses.hal.science/tel-03725400/document>.
- [54] B. J. Newton, Modelling of solar storage tanks, 1995. URL: <http://digital.library.wisc.edu/1793/7803>.
- [55] B. Baeten, T. Confrey, S. Pecceu, F. Rogiers, L. Helsen, A validated model for mixing and buoyancy in stratified hot water storage tanks for use in building energy simulations, *Applied Energy* 172 (2016) 217–229.
- [56] M. Michelsen, J. Villadsen, A convenient computational procedure for collocation constants, *The Chemical Engineering Journal* 4 (1972) 64–68.
- [57] E. Ebrahimzadeh, M. N. Shahrak, B. Bazooyar, Simulation of transient gas flow using the orthogonal collocation method, *Chemical Engineering Research and Design* 90 (2012) 1701–1710.
- [58] G. Carey, B. A. Finlayson, Orthogonal collocation on finite elements, *Chemical Engineering Science* 30 (1975) 587–596.
- [59] J. D. Hedengren, R. A. Shishavan, K. M. Powell, T. F. Edgar, Nonlinear modeling, estimation and predictive control in APMonitor, *Computers & Chemical Engineering* 70 (2014) 133–148.
- [60] D. R. Parida, S. Advaith, N. Dani, S. Basu, Assessing the impact of a novel hemispherical diffuser on a single-tank sensible thermal energy storage system, *Renewable Energy* 183 (2022) 202–218.
- [61] C. Xu, M. Liu, S. Jiao, H. Tang, J. Yan, Experimental study and analytical modeling on the thermocline hot water storage tank with radial plate-type diffuser, *International Journal of Heat and Mass Transfer* 186 (2022) 122478.
- [62] Gilbert F. Froment, Kenneth B. Bischoff, *Chemical Reactor Analysis and Design - Second Edition*, Wiley Series in Chemical Engineering, John Wiley and Sons, Inc, New York, 1990.